ACS APPLIED MATERIALS & INTERFACES

Research Article

www.acsami.org

Enhanced Radio Frequency Biosensor for Food Quality Detection Using Functionalized Carbon Nanofillers

Nicolas R. Tanguy,[†] Lindsey K. Fiddes,[‡] and Ning Yan*[,†,§]

[†]Faculty of Forestry, University of Toronto, 33 Willcocks Street, Toronto, Ontario M5S 3B3, Canada

[‡]Department of Mechanical and Industrial Engineering, University of Toronto, 5 King's College Road, Toronto, Ontario, M5S 3G8 Canada

[§]Department of Chemical Engineering and Applied Chemistry, University of Toronto, 200 College Street, Toronto, Ontario, M5S 3E5 Canada

ABSTRACT: This paper outlines an improved design of inexpensive, wireless and battery free biosensors for in situ monitoring of food quality. This type of device has an additional advantage of being operated remotely. To make the device, a portion of an antenna of a passive 13.56 MHz radio frequency identification (RFID) tag was altered with a sensing element composed of conductive nanofillers/particles, a binding agent, and a polymer matrix. These novel RFID tags were exposed to biogenic amine putrescine, commonly used as a marker for food spoilage, and their response was monitored over time using a general-purpose network analyzer. The effect of conductive filler properties, including conductivity and morphology, and filler functionalization was investigated by preparing sensing composites containing carbon particles (CPs), multiwall carbon nanotubes (MWCNTs), and binding agent grafted-multiwall carbon nanotubes (g-MWCNTs), respectively. During exposure to putrescine, the amount of reflected waves, frequency at resonance, and quality factor of the novel RFID tags decreased in response. The use of MWCNTs reduced tag cutoff time (i.e., faster response time) as compared with the use of CPs, which highlighted the effectiveness of the conductive nanofiller morphology, while the addition of g-MWCNTs further accelerated the sensor response time as a result of localized binding on the conductive nanofiller surface. Microstructural investigation of the film morphology indicated a better dispersion of g-MWCNTs in the sensing composite as compared to MWCNTs and CPs, as well as a smoother texture of the surface of the resulting coating. These results demonstrated that grafting of the binding agent onto the conductive particles in the sensing composite is an effective way to further enhance the detection sensitivity of the RFID tag based sensor.

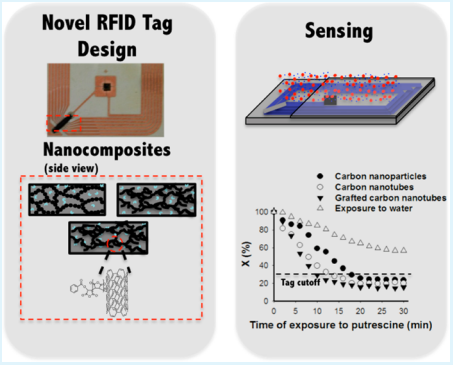

KEYWORDS: *RF communication, passive HF RFID tag, chemical sensor, food spoilage, nanocomposites, carbon nanotubes, chemical grafting*

INTRODUCTION

In the 21st century, detection and identification of gases in the environment are becoming crucial in response to the increasing awareness of the threat of chemical warfare agents, volatile organic compounds, and other biological molecules. However, traditionally used analytical techniques, such as gas chromatography,[1,2] ion mobility spectroscopy,[3] or mass spectrometry,[4,5] suffer from factors including the size of the instruments, price, and the need for specialized sample preparation and trained staff. The need for novel sensing devices that are rapid, robust, and cost-efficient and allow for real time monitoring is evident. As a result, there is an emergence of novel techniques that exploit advances in microelectronics and microfabrication techniques,[6,7] and/or use a biology-derived method.[8,9] The latter method imitates the olfactory sense of mammals and monitors the electrical, optical, or mechanical response of an array of receptors to a target, the volatile analyte. The identification of the analyte is then performed visually or by using a pattern recognition routine. The devices using this technique are referred to as electronic noses and have met considerable success owing to their low price, size, and energy consumption and have been applied to the detection of a large variety of vapors.[9−12]

The application of nanomaterials with high surface reactivity and dimensions approaching debye length have provided an exciting platform for developing electronic noses with enhanced sensitivity.[13] Accordingly, recent years have seen the emergence of a wide range of 0- or 1-dimensional nanomaterials that include nanoparticles,[14] nanowires,[15] nanotubes,[16] and graphene[17] as active elements in vapor sensors. In addition to the enhanced sensitivity, these materials offer various advantages such as fast response kinetics, superior stability, low power consumption, and low cost.[18] Also, functionalization of the surface of nanomaterials has provided a highly efficient method

Received: March 3, 2015
Accepted: May 20, 2015
Published: May 20, 2015

 © 2015 American Chemical Society

DOI: 10.1021/acsami.5b01876
ACS Appl. Mater. Interfaces 2015, 7, 11939−11947

to discriminate between analytes in complex vapor mixtures.[19] Among the previously mentioned nanomaterials, carbon nanotubes have attracted special attention owing to their superior electrical, thermal, and mechanical properties as compared with those of carbon nanoparticles,[20] which have promoted them as one promising nanomaterial for the next generation of gas sensors.

A step forward in real time and remote monitoring of gas composition in an environment was accomplished with the implementation of biosensors and electronic noses on radio frequency identification (RFID) transponders.[21−25] However, the previously developed methods suffer from either high power consumption,[21] or resulting devices with low coding capacity,[22−25] which hinder the large scale implementation due to the short lifetime of the device or due to the signal confusion in the case of simultaneous interrogation of multiple devices, respectively. In a simpler approach, truly passive RFID sensors with high coding capacity were fabricated by coating a material on the transponder antenna and during exposure to an analyte, with the change in dielectric or electrical properties of the coating affects the signal collected by the RFID reader.[26−30] The identification of the analyte is performed by exploiting the reflected signal characteristics and by using pattern recognition techniques. However, because of the need for an impedance analyzer or an oscilloscope, expensive sensing films such as Nafion or complex array of polymers associated with multivariate analysis remain barriers to the commercialization of these sensing devices.

In a previous study, a different approach was outlined, which uses the reflectance response of a novel design of a passive 13.56 MHz RFID tag that incorporates a conductive polymer composite (CPC) consisting of carbon particles (CPs), polyethylene vinyl acetate (PEVA), and maleic anhydride (MA) to identify and quantify a variety of volatile chemicals[31] and biogenic amines (BAs),[32] molecules generated during the process of food spoilage.[33] This method utilizes the changes in the composite electrical response over exposure to a volatile analyte resulting from the absorption of the analyte in the polymer matrix and the disruption of the conductive filler network. The change in electrical response of the composite material affects the response reflected back by the RFID tag, and above a certain threshold concentration of the analyte, the tag ceases to operate. Hence, with carefully tuning of the operating threshold according to the concentration of the analyte, sensors operating in a turn on/off basis that are simple, cost-effective, and wireless can be designed. These types of devices are of special importance for food spoilage monitoring in developing countries, in which food poisoning together with the ingestion of contaminated water caused the death of 1.8 million children in 1998, excluding China. In addition, cost-efficient food spoilage sensors would also help to reduce the medical costs related to foodborne illnesses in developed countries, evaluated as USD $6.5−34 billion in the USA in 1995. Although the previous devices successfully detected various BAs, they suffered from a long response time due to limited sensitivity. To alleviate these issues, two approaches can be considered: selecting a molecular recognition element with a higher partition coefficient and/or optimizing the transduction mechanism.

In this study, we investigated the effect of different carbon particles/nanomaterials of different properties including conductivity and morphology and the influence of grafting the binding agent on the surface of the nanomaterials on the transduction efficiency of the composite on the passive 13.56 MHz RFID tags sensor. Previous studies reported the difference in sensitivity between carbon materials with different morphology on the chemoresistive sensing performance of MWCNT/polymer composites,[34,35] and the functionalization of carbon surface with chemoselective polymers has been previously reported to increase the selectivity and sensitivity of carbon material composite to VOCs.[36] Since our detection system is composed of polymer matrix, binding agent, and conductive fillers, we hypothesize that the dimensions and electrical properties of the fillers as well as the functionalization of filler surface with the binding agent (MA) will affect the sensor sensitivity and response time toward putrescine. First, two previously reported methods, Diels−Alder reaction[37] and radical polymerization,[38] that were successful in grafting MA on carbon materials were tested. Then, three sensing composites, PEVA/MA/carbon particles (CPs), PEVA/MA/multiwall carbon nanotubes (MWCNTs), and PEVA/MA grafted-multiwall carbon nanotubes (g-MWCNTs), were coated on passive RIFD tags, and their response upon exposure to putrescine, a common BA, were characterized and compared. The morphologies of the different films were investigated using SEM, and some mechanisms were proposed to explain the behavior of the tag during exposure. Finally, the composite composed of g-MWCNTs was exposed to biogenic amines with a range of concentrations, and its sensitivity was compared to what was reported in some previous studies by our group.

EXPERIMENTAL SECTION

Materials. Salts of putrescine were received from Sigma-Aldrich (Oakville, ON) and used as received. CPs (graphitized, particle size <500 nm), MWCNTs (o.d. 10−15 nm, i.d. 2−6 nm, length 0.1−10 μm, >90% AS MWCNT), maleic anhydride, and poly(ethylene-*co*-vinyl acetate) (PEVA) (vinyl acetate 18 wt %) were purchased from Sigma-Aldrich (Oakville, ON) and used as received. Passive copper RFID tags (STMicroelectronics) operating at 13.56 MHz were purchased from Digi-Key Corporation (Thief River Falls, MN). Silicone elastomer kit was obtained from Dow Corning Corporation (Midland, MI).

Preparation of MA Grafted MWCNTs. Maleic anhydride was grafted on the MWCNT surface via Diels−Alder reaction and radical polymerization. Diels−Alder reaction was achieved by mixing 0.1 g of pristine MWCNTs and maleic anhydride in 20 mL of toluene and heating to 110 °C under reflux for 24 h. Radical polymerization was conducted by using BPO as polymerization reaction initiator. A 0.1 g portion of MWCNTs and maleic anhydride were placed in a three-neck flask with 20 mL of toluene and excess initiator. The mixture was heated to 110 °C for 8 h under reflux. Both reactions were conducted under nitrogen atmosphere to prevent side reactions. Reacted MWCNTs were collected using a crucible (medium size), and the unreacted maleic anhydride was washed away via Soxhlet extraction with boiling toluene for 24 h. Modified MWCNTs were then oven-dried at 65 °C prior to further testing.

Grafted Filler Characterization. Thermal stability of pristine and modified MWCNTs was investigated using a thermal gravimetric analyzer (TGA, TA TGA-Q500, TA Instruments). TGA was used for its ease in estimating grafting yield. A 10 mg portion of material was placed in a platinum pan and heated up to 600 °C with a heating rate of 10 °C/min under nitrogen. Surface characteristics of pristine MWCNTs and modified MWCNTs were investigated via zeta potential analysis (Zeta Plus, Brookhaven Instrument Corporation). The 10 mg portions of pristine MWCNTs and grafted MWCNTs were dispersed in 20 mL of water, and the zeta potential was calculated as an average of 10 measurements. Mixtures were sonicated for 5 min and left standing 30 min prior to testing. Surface functional groups for pristine MWCNTs and modified MWCNTs were investigated by

DOI: 10.1021/acsami.5b01876
ACS Appl. Mater. Interfaces 2015, 7, 11939−11947

FTIR (400 cm^{-1} to 4000 cm^{-1}). A 2 mg portion of carbon nanofillers was mixed with 200 mg of oven-dried KBr, which was then pelletized and tested. The morphology of the composites coated on the RFID tag was investigated by scanning the surface of the films using a Hitachi S-5200 scanning electron microscope (SEM).

Device Fabrication. Passive RFID tags operating at 13.56 MHz frequency were used as the sensor substrate and the antenna altered following previously developed methods with slight modifications.[31,32] RFID tags were coated with composites composed of conductive fillers (CPs, MWCNTs, and g-MWCNTs), poly(ethylene-*co*-vinyl acetate), and maleic anhydride at weight percentages of 18%/32%/50% or 50%/50%. Mixtures were dissolved in 15 mL of dichlorobenzene and sonicated for 1 h at room temperature to ensure homogeneity. In this procedure, the silver paste was left intact while in the previously reported procedure a thin layer of paste was removed with tape. Final target tag resistance was of 5.0 ± 1.0 Ω after applying multiple layers of the composites. After modification of the RFID tags, the operating frequency was found to increase from 13.56 to 14.20 MHz.

Biogenic Amine Detection. A general-purpose network analyzer (PNA, Agilent HPE8361A) working in frequencies ranging from 10 to 16 MHz was used to monitor tag response after exposure to putrescine. The PNA was equipped with a single coil copper antenna, and the tag/antenna array was placed in a Petri dish containing 40 mL of putrescine solution. The PNA antenna was placed at 5 mm from the Petri dish lid. A putrescine solution of 0.25 M was then added and heated to 35 °C, and the tag responses were recorded every 2 min for 30 min. Samples were repeated in triplicate to generate error bars.

Tag Operating Principle. In our experiments, the silver paste on the bottom right of the tag is partially replaced with the composite material; as such, the RFID tag equivalent circuit can be modeled as shown in Figure 1.

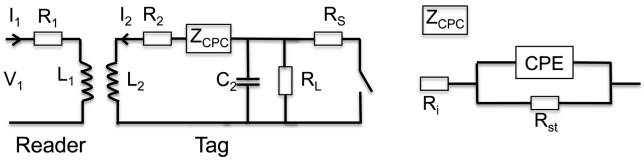

Figure 1. Equivalent circuit of the novel RFID tag design.

By assuming that the changes in electrical properties of the composite over exposure to amines are mainly resistive, due to increased distance between conductive fillers, the novel tag impedance and quality factor can be derived as follows:

$$Z_{tag} = \frac{\frac{R_2}{R_L} + \frac{R_i}{R_L} + jw\left(\frac{L_2}{R_L} + R_L + R_2\right) - w^2 L_2 C_2 + 1}{\frac{1}{R_L} + jwC_2} \quad (1)$$

By assuming that, at resonance, the antenna of the tag capacitive element is related to the antenna inductance, we obtain

$$C_2 = \frac{1}{w_0^2 L_2} \quad (2)$$

Hence, the novel tag quality factor (Q) can be expressed as

$$Q = \left(\frac{w_0 L_2}{R_L} + \frac{R_i}{w_0 L_2} + \frac{R_2}{w_0 L_2}\right)^{-1} \quad (3)$$

Thus, the quality factor determined experimentally can be used to obtain the variation in PEVA/MA/conductive filler composite response using eq 3.

RESULTS AND DISCUSSION

Preparation of Functionalized MWCNTs. In this study, two grafting methods were explored to attach MA molecules on the surface of MWCNTs. The Diels–Alder reaction, also referred to as "click reaction", allows grafting individual molecules of MA on the surface of MWCNTs without inserting other components beside the solvent, as shown in Figure 2. In

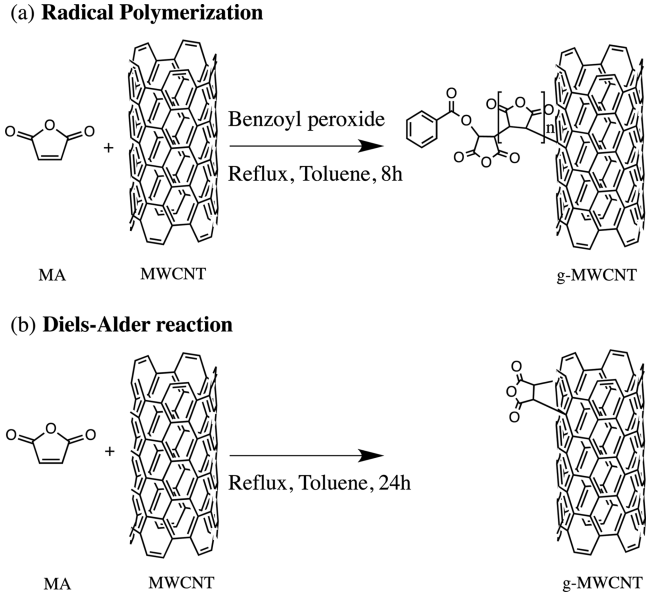

Figure 2. (a) Radical polymerization of MA on MWCNTs. (b) Diels–Alder reaction of MA on MWCNTs.

this reaction, MA would act as a diene while MWCNTs would act as dienophile. In contrast, radical polymerization of MA on the surface of MWCNTs requires the addition of benzoyl peroxide to initiate the reaction and results in grafting long chains of MA on the MWCNTs surface.

Following the MWCNT grafting and washing stages, qualitative and quantitative investigation of the effectiveness of the grafting reactions were conducted. FTIR and zeta potential analysis were used to confirm the grafting of MA on MWCNTs, while TGA characterization provided an estimate of the amount of material grafted.

Pristine MWCNTs and functionalized MWCNTs were characterized by FTIR, as shown in Figure 3b. Characteristic functional groups for pristine MWCNTs and functionalized MWCNTs have been reported previously. The absorption band of pristine MWCNTs at 3400 cm^{-1} is characteristic of the —OH group stretching, which may be due to MWCNT residual impurities or humidity, while absorption bands in the 1475–1600 cm^{-1} region can be assigned to the MWCNTs' aromatic C=C stretching. FTIR spectra of modified MWCNTs revealed different functional groups, with the emergence of absorption bands at 2928, 2859, and 1744 cm^{-1}, which are characteristic of $—CH_2—$ stretching and C=O stretching.[39] These results suggest that MA was successfully grafted on the MWCNTs' surface. It can be noted that MWCNTs functionalized through radical polymerization had more intense absorption bands at wavelengths characteristics of MA functional groups. To confirm the grafting of MA on MWCNTs, the zeta potential of MWCNTs before and after functionalization was measured. Table 1 summarizes the zeta potential values for pristine MWCNTs and functionalized MWCNTs dispersed in water. The negative zeta potential of pristine MWCNTs could be due to the presence of residual hydroxyl or carboxyl groups on the surface. Grafting negatively charged molecules on the surface of MWCNTs, such as MA, should further reduce the zeta potential of the modified filler.[40] Higher surface charge

DOI: 10.1021/acsami.5b01876
ACS Appl. Mater. Interfaces 2015, 7, 11939–11947

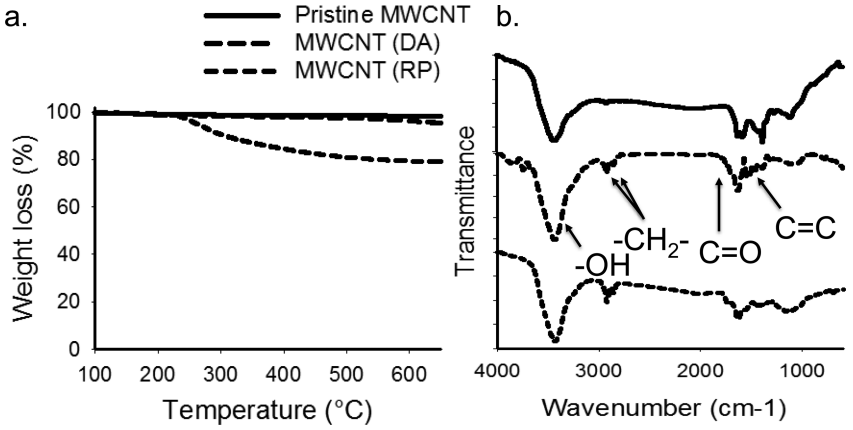

Figure 3. (a) TGA thermographs and (b) FTIR spectra of pristine MWCNTs and modified MWCNTs via Diels–Alder reaction (DA) and radical polymerization (RP).

Table 1. Zeta Potential of the Nanofillers

fillers	zeta potential (mV)
pristine MWCNT	−19.57 ± 4.9
MWCNT (Diels–Alder)	−25.00 ± 3.5
MWCNT (radical polymerization)	−35.01 ± 2.1

indicates an increased repulsion force between the medium (water) and the particles (MWCNTs and g-MWCNTs), which corresponds to a more stable dispersion system,[41] and further confirms the grafted MA on the surface of the MWCNTs.

The percentage of MA grafted, as determined by TGA, is shown in Figure 3a. The degradation of organic fractions on grafted MWCNTs usually occurs from 250 to 500 °C.[42−44] MA was reported to fully degrade at temperatures below 200 °C. The thermal degradation profile of pristine MWCNTs did not reveal obvious mass loss at temperatures below 500 °C, while the degradation of functionalized MWCNTs started at 200 °C. It indicates that the mass loss likely resulted from the grafted

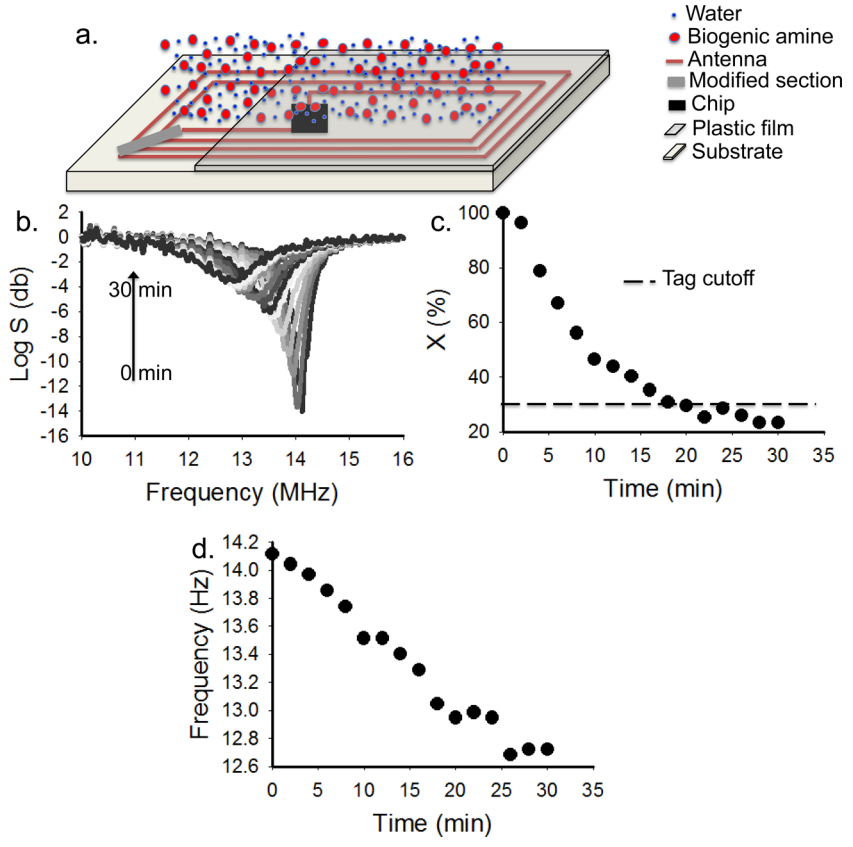

Figure 4. (a) Representation of the novel RFID tag during exposure to a putrescine solution. Typical reflectance characteristics of a modified RFID tag are shown. (b) Log plot of the amount of signal reflected from 10 to 16 MHz during exposure to BA. (c) Plot showing the relative amount of radio waves reflected over time for the modified tag. The dashed line in part c represents the cutoff, which occurs when less than 30% of the relative amount of radio waves is reflected back to the network analyzer. (d) Plot showing the frequency at resonance over time for the modified tag.

DOI: 10.1021/acsami.5b01876
ACS Appl. Mater. Interfaces 2015, 7, 11939−11947

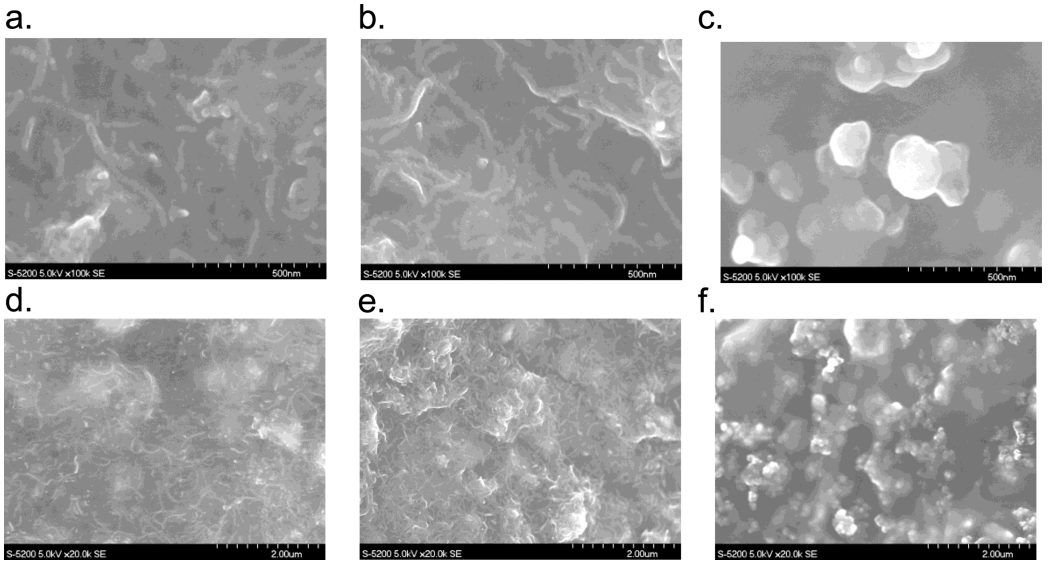

Figure 5. SEM pictures of the 3 films coated on RFID tags: (a, d) g-MWCNTs composite, (b, e) MWCNTs composite, and (c, f) CPs composite.

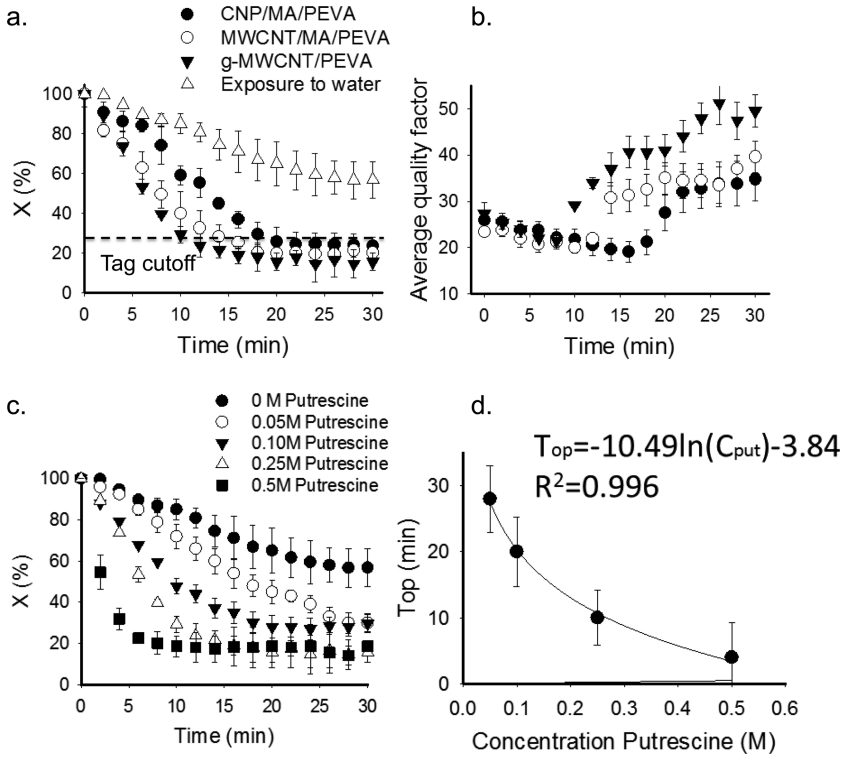

Figure 6. Evolution of (a) relative amplitude and (b) average quality factor of tags coated with composites composed of CPs, MWCNTs, and g-MWCNTs as conductive fillers during exposure to 0.25 M putrescine and water. Evolution of (c) relative amplitude and (d) time at which the tag ceases to operate for composites of g-MWCNTs during exposure to different putrescine concentration.

MA. Thermal degradation of Diels–Alder reacted MWCNTs and radical polymerization reacted MWCNTs occurred at 450 and 250 °C, respectively. This difference may be related to the formation of one or two covalent bonds between MA and the surface of MWCNTs in radical polymerization reaction and in Diels–Alder reaction, respectively. Nevertheless, these results allow the estimation of the mass fraction of MA grafted using both reactions. It was found that 5 and 20 wt % of MA were grafted on the surface of MWCNTs after performing Diels–Alder reaction and radical polymerization, respectively. The amounts fell within the range of previously reported grafting yield of MA on the surface of MWCNTs by radical polymerization, 10–25 wt %,[45,46] and Diels–Alder reaction, 5–10 wt %.[37]

Sensor Operating Principle. Passive RFID tags were coated with the composite material composed of PEVA, selected for its weak ability to swell upon exposure to water, and carbon nanofillers, used to generate a semiconductive material. MA was added in the composite to act as a binding agent toward BA.[47] Binding or interactions between MA and BA result in the progressive swelling of the polymer matrix over time. In turn, the swelling of the polymer affects the network of

DOI: 10.1021/acsami.5b01876
ACS Appl. Mater. Interfaces 2015, 7, 11939–11947

fillers, and thus the electrical response of the CPC, which transduces changes in the reflectance characteristics of the RFID tags. The reflectance characteristics of an RFID transponder can be expressed in terms of frequency at resonance, *F* Hz, and the relative amount of radio waves reflected, *X*%. They were both monitored in this study during the exposure of the RFID transponder tag to BA for 30 min using a general purpose network analyzer.

Figure 4a illustrates an RFID sensor exposed to a solution of putrescine while Figure 4b−d shows the response of an RFID sensor during exposure to a solution of 0.25 M putrescine for 30 min. As the CPC film absorbs BA, its electrical response changes, which further affects the impedance of the transponder's antenna and induces changes in the reflected response signal. These fluctuations reduce both the frequency at resonance and the relative amount of radio waves reflected by the tag, as shown in Figure 4c,d. When only 30% or less relative amount of radio waves is reflected, the RFID transponder is considered as inoperable as the reflected radio frequency signal from the tag is not detectable by the reader. Hence, results for the novel tag shown in Figure 4 reveal that after 20 min of exposure to 0.25 M putrescine the tag was inoperable.

Morphology of the Coated Films. The morphology of the composite films coated on RFID tags was investigated using SEM; pictures are shown in Figure 5. There were no significant microstructural differences observed between MWCNTs and g-MWCNTs at high magnifications, as shown in Figure 5a,b. However, Figure 5d,e indicates a better distribution of the conductive fillers in the g-MWCNT composite as compared to MWCNTs. In addition, the surface of the g-MWCNTs coating was found to be smoother than that of the MWCNT and CP composite, which could be due to a better compatibility between the conductive fillers and the matrix resulting from the grafting of MA at the surface of the conductive fillers.[45] Previous studies have reported the importance of the microstructure and nanostructure of CPCs on the sensitivity toward volatile analytes.[48,49] It was suggested that the swelling of the matrix resulting from the sorption of the analyte in the matrix causes the disruption of the conductive network, and thus a chemoelectrical response of the device. Hence, achieving a good dispersion of conductive fillers in the matrix is crucial to optimize the sensitivity of CPCs toward volatile compounds as a better dispersion facilitates the disruption of the conductive network during exposure to volatile compounds and enhance the sensitivity of the device.[50,51]

Influence of Filler Type on the Sensitivity of the RFID Sensors. The effect of CP, MWCNT, and g-MWCNT (radical polymerization) composites on the sensitivity of the novel type of RFID tags after exposure to 0.25 M putrescine is shown in Figure 6a,b. A response to water was observed for the relative amplitude of the coated tags. These results suggest that some level of background noise exists due to interference by water and the heat generated during the experiments. However, the tags have achieved a good level of signal-to-noise ratio to be considered effective for the intended application.[32] An overall faster response time by a factor of 2 was obtained due to the change in the procedure of RFID tag preparation,[32] and both changing the filler type and using grafting instead of blending for MA affected the tag cutoff time. Tags with PEVA/MA/CPs, PEVA/MA/MWCNTs, and PEVA/g-MWCNTs had 20, 14, and 10 min as the cutoff time, respectively. Less cutoff time indicates a quicker or more sensitive response. It is likely that the inoperability of the tag is related to the increase in the resistance of the tag antenna, which induces a mismatch between the antenna and the chip impedance, as shown in eq 3. Hence, in the case of PEVA/g-MWCNTs, the less time to reach cutoff intrinsically is related to a faster increase of the resistance of the sensing composite material. With consideration of filler size and morphology, a higher initial conductivity and a more complex network are obtained when similar amounts of MWCNTs are added as compared to samples with CPs.[52] However, the opposite outcome was previously reported, with an increase in sensitivity by a factor 4 with blending carbon black in poly(styrene-*co*-butadyene) as compared to that with MWCNTs poly(styrene-*co*-butadyene).[34] This phenomenon may be related to the presence of a binding agent (MA) in our system in addition to the matrix and the conductive fillers, while the system reported in the literature study only comprised a polymeric matrix and conductive fillers. Thus, different synergies between MA and MWCNT and CP in the composites could lead to this outcome. In addition, a larger amount of PEVA/MA/CPs is needed for the tag to reach 5 Ω, as compared with PEVA/MA/MWCNTs. This resulted in a composite of lower thickness for the latter, and thus an increased diffusion flow of putrescine (J) into the composite film, following Fick's first law of diffusion.[53] This outcome could also be due to additional transduction mechanisms in the current system rather than purely chemoresistive sensing taking place. By grafting MA on MWCNTs, the tag cutoff time was further reduced. This phenomenon is likely due to the more homogeneous dispersion of the conductive network in g-MWCNTs films, as previously mentioned, and to the presence of BA at the surface of the conductive filler, as shown in Figure 7. In Figure 7a, MA is

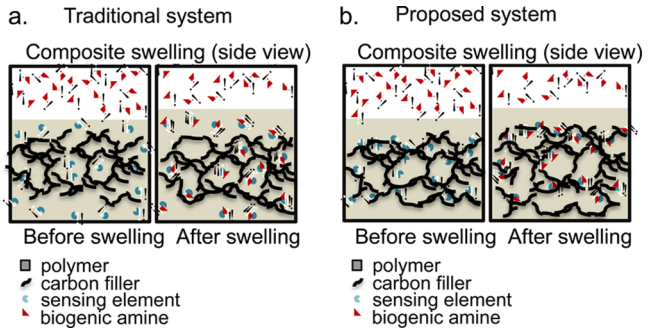

Figure 7. Illustration of (a) blended MWCNTs/MA/PEVA and (b) grafted MA on MWCNT/PEVA detection principle of BA.

blended into the composite, and thus binding with BA will induce a localized swelling; nevertheless, the distance gap between MA and MWCNTs makes the disruption of the conductive network less effective. In contrast, in Figure 7b, binding of BA occurs at the surface of the MWCNTs, and thus results in the larger disruption of the network faster. With increasing the concentration of putrescine during exposure, the tag cutoff time was reduced, as shown in Figure 6c. Cutoff times were of 4, 10, 20, and 28 min with exposure to 0.5, 0.25, 0.1, and 0.05 M of putrescine, respectively. The sensitivity of the composite of g-MWCNTs was further determined by plotting the time at which the tags cease to operate (T_{op}) against the concentration in putrescine during tag exposure, as shown in Figure 5d. It was found that the T_{op} followed a logarithmic decay with increasing the concentration in putrescine during

DOI: 10.1021/acsami.5b01876
ACS Appl. Mater. Interfaces 2015, 7, 11939−11947

exposure, confirming the previously reported results.[32] The relationship between T_{op} and putrescine concentration was $T_{op} = -10.49 \ln(C_{put}) - 3.84$, which reveals a faster cutoff of the tags with g-MWCNTs composites as compared to that of previously reported for composites of CPs, $T_{op} = -20.77 \ln(C_{put}) + 31.62$.[32]

The average quality factor for the tags containing the three types of sensing composites after exposure to 0.25 M putrescine solutions is shown in Figure 6b. The initial quality factor of the RFID tags was between 23 and 27, which falls in the range for operating RFID devices.[54] After being exposed to putrescine, the RFID tags quality factor decreased first prior to a steady increase. The quality factor for the PEVA/MA/CPs, PEVA/MA/MWCNTs, and PEVA/g-MWCNTs composites showed a minimum at 16, 10, and 8 min, respectively. In the first stage, the quality factor decreased, which highlights an increase in the bandwidth of the transponder. During exposure to putrescine, the shift from semiconductive to insulating material results in an increase of the RFID tag bandwidth as suggested in eq 3. The quicker increase of the quality factor when using MWCNTs and g-MWCNTs compared to CPs composites indicates a quicker increase in the signal bandwidth, which agrees with the previously obtained results. The transition from first to second stage is likely due to the inoperability of the tag, as the signal maximum intensity approaches −3 dB. As such, the higher Q factor does not convey a reduction in the signal bandwidth but the inoperability of the tag itself.

CONCLUSION

Finding novel techniques that are cost-effective, simple, and noninvasive for food quality monitoring is crucial for developing countries. In this paper, we present the use of novel inexpensive passive 13.56 MHz RFID tags to detect and quantify the amount of putrescine, a common biogenic amine byproduct generated during food spoilage. Passive RFID tags were altered using CPCs composed of different types of conductive nanofillers (MWCNTs, CPs, and g-MWCNTs), a sensing agent (MA), and a polymer matrix (PEVA). Diels–Alder reaction and radical polymerization were used to graft MA on MWCNTs. With radical polymerization, the grafting yield was higher, and the zeta potential of the nanomaterials was lower, as compared to the Diels–Alder reaction. The novel tags were then exposed to putrescine vapor, and tag response in terms of relative amount of reflected waves, frequency at resonance, and quality factor were monitored over time using a network analyzer. Tags became inoperable after 20, 14, and 10 min exposure when using CPs, MWCNTs, and g-MWCNTs as the conductive fillers, respectively, with less time indicating a higher sensitivity. RFID tag quality factor was determined experimentally and shown to first decrease as a result of the increased tag resistance and then increase due to the tag becoming inoperable. This study demonstrated that MWCNTs and grafted MWCNTs can be used to make more sensitive RFID tags capable of faster detection/sensing of spoilage in food. Future work will focus on the investigation of the difference in synergy between MA and CPs/MWCNTs, testing the sensors against interfering substances and the elucidation of the nature of the electrical response of the composite resulting in RFID tags cutoff.

AUTHOR INFORMATION

Corresponding Author

*Phone: +1(416)-946-8070. Fax: +1(416)-978-3834 E-mail: ning.yan@utoronto.ca.

Notes

The authors declare no competing financial interest.

ACKNOWLEDGMENTS

The authors are grateful to the Sentinel: Bioactive Paper Network (Canada) for their financial support. The authors would like to thank Tse V. Chan, Photonics/Microwave Lab Manager, Electrical and Computer Engineering, University of Toronto, for providing the access to the network analyzer and for providing his invaluable suggestions. The authors would also like to acknowledge Thierry KM, Peiyu Kuo, and Rosanna Kronfi at the Faculty of Forestry, University of Toronto, for their support.

REFERENCES

(1) Popiel, S.; Sankowska, M. Determination of Chemical Warfare Agents and Related Compounds in Environmental Samples by Solid-Phase Microextraction with Gas Chromatography. *J. Chromatogr. A* **2011**, *1218*, 8457–8479.

(2) Jia, M.; Koziel, J.; Pawliszyn, J. Fast Field Sampling/Sample Preparation and Quantification of Volatile Organic Compounds in Indoor Air by Solid-Phase Microextraction and Portable Gas Chromatography. *Field Anal. Chem. Technol.* **2000**, *4*, 73–84.

(3) Borsdorf, H.; Mayer, T.; Zarejousheghani, M.; Eiceman, G. A. Recent Developments in Ion Mobility Spectrometry. *Appl. Spectrosc. Rev.* **2011**, *46*, 472–521.

(4) Kientz, C. E. Chromatography and Mass Spectrometry of Chemical Warfare Agents, Toxins and Related Compounds: State of the Art and Future Prospects. *J. Chromatogr. A* **1998**, *814*, 1–23.

(5) Fortner, E. C.; Zheng, J.; Zhang, R.; Berk Knighton, W.; Volkamer, R. M.; Sheehy, P.; Molina, L.; André, M. Measurements of Volatile Organic Compounds Using Proton Transfer Reaction—Mass Spectrometry During the MILAGRO 2006 Campaign. *Atmos. Chem. Phys.* **2009**, *9*, 467–481.

(6) Lu, C.-J.; Steinecker, W. H.; Tian, W.-C.; Oborny, M. C.; Nichols, J. M.; Agah, M.; Potkay, J. A.; Chan, H. K. L.; Driscoll, J.; Sacks, R. D.; Wise, K. D.; Pang, S. W.; Zellers, E. T. First-Generation Hybrid MEMS Gas Chromatograph. *Lab Chip* **2005**, *5*, 1123–1131.

(7) Miller, R. A.; Nazarov, E. G.; Eiceman, G. A.; Thomas King, A. A MEMS Radio-Frequency Ion Mobility Spectrometer for Chemical Vapor Detection. *Sens. Actuators, A* **2001**, *91*, 301–312.

(8) Persaud, K.; Dodd, G. Analysis Of Discrimination Mechanisms in The Mammalian Olfactory System Using a Model Nose. *Nature* **1982**, *299*, 352–355.

(9) Rakow, N. A.; Suslick, K. S. A Colorimetric Sensor Array for Odour Visualization. *Nature* **2000**, *406*, 710–713.

(10) Pejcic, B.; Crooke, E.; Boyd, L.; Doherty, C. M.; Hill, A. J.; Myers, M.; White, C. Using Plasticizers To Control the Hydrocarbon Selectivity of a Poly(methyl methacrylate)-Coated Quartz Crystal Microbalance Sensor. *Anal. Chem.* **2012**, *84*, 8564–8570.

(11) Tung, T. T.; Castro, M.; Pillin, I.; Kim, T. Y.; Suh, K. S.; Feller, J. F. Graphene-Fe3O4/PIL-PEDOT for the Design of Sensitive and Stable Quantum Chemo-Resistive VOC Sensors. *Carbon* **2014**, *74*, 104–112.

(12) Gan, H. L.; Man, Y. B. C.; Tan, C. P.; NorAini, I.; Nazimah, S. A. H. Characterisation of Vegetable Oils by Surface Acoustic Wave Sensing Electronic Nose. *Food Chem.* **2005**, *89*, 507–518.

(13) Mao, S.; Ganhua, L.; Chen, J. Nanocarbon-Based Gas Sensors: Progress and Challenges. *J. Mater. Chem. A* **2014**, *2*, 5573–5579.

(14) Suematsu, K.; Shin, Y.; Hua, Z.; Yoshida, K.; Yuasa, M.; Kida, T.; Shimanoe, K. Nanoparticle Cluster Gas Sensor: Controlled

DOI: 10.1021/acsami.5b01876
ACS Appl. Mater. Interfaces 2015, 7, 11939–11947

Clustering Of SnO2 Nanoparticles for Highly Sensitive Toluene Detection. *ACS Appl. Mater. Interfaces* **2014**, *6*, 5319−5326.
(15) Park, W. J.; Choi, K. J.; Kim, M. H.; Koo, B. H.; Lee, J. L.; Baik, J. M. Self-Assembled and Highly Selective Sensors Based on Air-Bridge-Structured Nanowire Junction Arrays. *ACS Appl. Mater. Interfaces* **2013**, *5*, 6802−6807.
(16) Kim, D. H.; Shim, Y.; Jeon, J.; Jeong, H. Y.; Park, S. S. Vertically Ordered Hematite Nanotube Array as an Ultrasensitive and Rapid Response Acetone Sensor. *ACS Appl. Mater. Interfaces* **2014**, *6*, 6−11.
(17) Kumar, B.; Min, K.; Bashirzadeh, M.; Farimani, A. B.; Bae, M. H.; Estrada, D.; Kim, Y. D.; Yasaei, P.; Park, Y. D.; Pop, E.; Aluru, N. R.; Salehi-Khojin, A. The Role of External Defects in Chemical Sensing of Graphene Field-Effect Transistors. *Nano Lett.* **2013**, *13*, 1962−1968.
(18) Wilson, A. .; Baietto, M. Applications and Advances in Electronic-Nose Technologies. *Sensors* **2009**, *9*, 5099−5148.
(19) Wei, L.; Shi, D.; Ye, P.; Dai, Z.; Chen, H.; Chen, C.; Wang, J.; Zhang, L.; Xu, D.; Wang, Z.; Zhang, Y. Hole Doping and Surface Functionalization of Single-Walled Carbon Nanotube Chemiresistive Sensors for Ultrasensitive and Highly Selective Organophosphor Vapor Detection. *Nanotechnology* **2011**, *22*, 425501.
(20) Ajayan, P. M. Nanotubes From Carbon. *Chem. Rev.* **1999**, *99*, 1787−1800.
(21) Mascaro, D. J.; Baxter, J. C.; Halvorsen, a.; White, K.; Scholz, B.; Schulz, D. L. ChemiBlock Transducers. *Sens. Actuators, B* **2007**, *120*, 353−361.
(22) Ogi, H.; Nagai, H.; Fukunishi, Y.; Yanagida, T.; Hirao, M.; Nishiyama, M. Multichannel Wireless-Electrodeless Quartz-Crystal Microbalance Immunosensor. *Anal. Chem.* **2010**, *82*, 3957−3962.
(23) Cai, Q.; Zeng, K.; Ruan, C.; Desai, T. A.; Grimes, C. A. A Wireless, Remote Query Glucose Biosensor Based on a pH-Sensitive Polymer. *Anal. Chem.* **2004**, *76*, 4038−4043.
(24) Lu, Q.; Lin, H.; Ge, S.; Luo, S.; Cai, Q.; Grimes, C. A. Wireless, Remote-Query, and High Sensitivity Escherichia Coli O157:H7 Biosensor Based on the Recognition Action of Concanavalin A. *Anal. Chem.* **2009**, *81*, 5846−5850.
(25) Ogi, H.; Fukunishi, Y.; Omori, T.; Hatanaka, K.; Hirao, M.; Nishiyama, M. Effects of Flow Rate on Sensitivity and Affinity in Flow Injection Biosensor Systems Studied by 55-MHz Wireless Quartz Crystal Microbalance. *Anal. Chem.* **2008**, *80*, 5494−5500.
(26) Potyrailo, R. a; Nagraj, N.; Surman, C.; Boudries, H.; Lai, H.; Slocik, J. M.; Kelley-Loughnane, N.; Naik, R. R. Wireless Sensors and Sensor Networks for Homeland Security Applications. *TrAC, Trends Anal. Chem.* **2012**, *40*, 133−145.
(27) Potyrailo, R. A.; Surman, C.; Morris, W. G.; Go, S.; Lee, Y.; Cella, J.; Chichak, K. S. Selective Quantitation of Vapors and Their Mixtures Using Individual Passive Multivariable RFID Sensors. *Conf. Proc. Int. IEEE Conf. RFID* **2010**, 22−28.
(28) Potyrailo, R. A.; Nagraj, N.; Tang, Z.; Mondello, F. J.; Surman, C.; Morris, W. Battery-Free Radio Frequency Identification (RFID) Sensors for Food Quality and Safety. *J. Agric. Food Chem.* **2012**, *60*, 8535−8543.
(29) Potyrailo, R. A.; Surman, C.; Nagraj, N.; Burns, A. Materials and Transducers toward Selective Wireless Gas Sensing. *Chem. Rev.* **2011**, *111*, 7315−7354.
(30) Loh, K. J.; Lynch, J. P.; Kotov, N. A. Inductively Coupled Nanocomposite Wireless Strain and pH Sensors. *Smart Struct. Syst.* **2008**, *4*, 531−548.
(31) Fiddes, L. K.; Yan, N. RFID Tags for Wireless Electrochemical Detection of Volatile Chemicals. *Sens. Actuators, B* **2013**, *186*, 817−823.
(32) Fiddes, L. K.; Chang, J.; Yan, N. Electrochemical Detection of Biogenic Amines During Food Spoilage Using an Integrated Sensing RFID Tag. *Sens. Actuators, B* **2014**, *202*, 1298−1304.
(33) Silla Santos, M. H. Biogenic Amines: Their Importance In Foods. *Int. J. Food Microbiol.* **1996**, *29*, 213−231.
(34) Covington, J. A.; Gardner, J. W. Carbon Nanomaterial Polymer Composite ChemFET and Chemoresistors for Vapour Sensing. *AIP Conf. Proc.* **2009**, *1137*, 38−41.
(35) Sakale, G.; Jakovlevs, D.; Aulika, I.; Knite, M. Effect of Nanotube Aspect Ratio on Chemical Vapour Sensing Properties of Polymer/MWCNT Composites. *J. Nano Res.* **2012**, *21*, 117−123.
(36) Nag, S.; Duarte, L.; Bertrand, E.; Celton, V.; Castro, M.; Choudhary, V.; Guegan, P.; Feller, J.-F. Ultrasensitive QRS Made by Supramolecular Assembly of Functionalized Cyclodextrins and Graphene for the Detection of Lung Cancer VOC Biomarkers. *J. Mater. Chem. B* **2014**, *2*, 6571−6579.
(37) Munirasu, S.; Albuerne, J.; Boschetti-de-Fierro, A.; Abetz, V. Functionalization of Carbon Materials Using the Diels-Alder Reaction. *Macromol. Rapid Commun.* **2010**, *31*, 574−579.
(38) Zhou, X.; Li, Q.; Wu, C. Grafting of Maleic Anhydride onto Carbon Black Surface via Ultrasonic Irradiation. *Appl. Organomet. Chem.* **2008**, *22*, 78−81.
(39) Xu, P.; Cui, D.; Pan, B.; Gao, F.; He, R.; Li, Q.; Huang, T.; Bao, C.; Yang, H. A Facile Strategy for Covalent Binding of Nanoparticles onto Carbon Nanotubes. *Appl. Surf. Sci.* **2008**, *254*, 5236−5240.
(40) Sun, Z.; Nicolosi, V.; Rickard, D.; Bergin, S. D.; Aherne, D.; Coleman, J. N. Quantitative Evaluation of Surfactant-Stabilized Single-Walled Carbon Nanotubes: Dispersion Quality and Its Correlation with Zeta Potential. *J. Phys. Chem. C* **2008**, *112*, 10692−10699.
(41) White, B.; Banerjee, S.; O'Brien, S.; Turro, N. J.; Herman, I. P. Zeta-Potential Measurements of Surfactant-Wrapped Individual Single-Walled Carbon Nanotubes. *J. Phys. Chem. C* **2007**, *111*, 13684−13690.
(42) Dyke, C. A.; Tour, J. M. Unbundled and Highly Functionalized Carbon Nanotubes from Aqueous Reactions. *Nano Lett.* **2003**, *3*, 1215−1218.
(43) Liu, I. C.; Huang, H. M.; Chang, C. Y.; Tsai, H. C.; Hsu, C. H.; Tsiang, R. C. C. Preparing a Styrenic Polymer Composite Containing Well-Dispersed Carbon Nanotubes: Anionic Polymerization of a Nanotube-Bound P-methylstyrene. *Macromolecules* **2004**, *37*, 283−287.
(44) Chen, S.; Shen, W.; Wu, G.; Chen, D.; Jiang, M. A New Approach to the Functionalization of Single-Walled Carbon Nanotubes with Both Alkyl and Carboxyl Groups. *Chem. Phys. Lett.* **2005**, *402*, 312−317.
(45) Wu, H. L.; Wang, C. H.; Ma, C. C. M.; Chiu, Y. C.; Chiang, M. T.; Chiang, C. L. Preparations and Properties of Maleic Acid and Maleic Anhydride Functionalized Multiwall Carbon Nanotube/Poly(urea urethane) Nanocomposites. *Compos. Sci. Technol.* **2007**, *67*, 1854−1860.
(46) Wu, X.; Liu, P. Polymer Grafted Multiwalled Carbon Nanotubes via Facile in Situ Solution Radical Polymerization. *J. Exp. Nanosci.* **2010**, *5*, 383−389.
(47) Butler, P. J.; Harris, J. I.; Hartley, B. S.; Lebeman, R. The Use of Maleic Anhydride for the Reversible Blocking of Amino Groups in Polypeptide Chains. *Biochem. J.* **1969**, *112*, 679−689.
(48) Feller, J. F.; Langevin, D.; Marais, S. Influence of Processing Conditions on Sensitivity of Conductive Polymer Composites to Organic Solvent Vapours. *Synth. Met.* **2004**, *144*, 81−88.
(49) Feller, J. F.; Grohens, Y. Electrical Response of Poly(styrene)/Carbon Black Conductive Polymer Composites (CPC) To Methanol, Toluene, Chloroform and Styrene Vapors as a Function of Filler Nature and Matrix Tacticity. *Synth. Met.* **2005**, *154*, 193−196.
(50) Castro, M.; Lu, J.; Bruzaud, S.; Kumar, B.; Feller, J. F. Carbon Nanotubes/Poly(ε-caprolactone) Composite Vapour Sensors. *Carbon* **2009**, *47*, 1930−1942.
(51) Wang, H. C.; Li, Y.; Yang, M. J. Sensors for Organic Vapor Detection Based on Composites of Carbon Nonotubes Functionalized with Polymers. *Sens. Actuators, B* **2007**, *124*, 360−367.
(52) Sumfleth, J.; Buschhorn, S. T.; Schulte, K. Comparison of Rheological and Electrical Percolation Phenomena in Carbon Black and Carbon Nanotube Filled Epoxy Polymers. *J. Mater. Sci.* **2011**, *46*, 659−669.
(53) George, S. C.; Thomas, S. Transport Phenomena through Polymeric Systems. *Prog. Polym. Sci.* **2001**, *26*, 985−1017.

DOI: 10.1021/acsami.5b01876
ACS Appl. Mater. Interfaces 2015, 7, 11939−11947

(54) Reinhold, C.; Scholz, P.; John, W.; Hilleringmann, U. Efficient Antenna Design of Inductive Coupled RFID-Systems with High Power Demand. *J. Commun.* **2007**, *2* (6), 14−23.

DOI: 10.1021/acsami.5b01876
ACS Appl. Mater. Interfaces 2015, 7, 11939−11947